

Fluorobenzoic Acids Coformers to Improve the Solubility and Permeability of BCS Class IV Drug Naftopidil

M. K. Chaitanya Mannava,^{a,b} Manish K. Bommaka,^a Rambabu Dandela,^{c,d} K. Anand Solomon,^b Ashwini K. Nangia^{*,a,c}

^a School of Chemistry, University of Hyderabad, Prof. C. R. Rao Road, Gachibowli, Central University P.O., Hyderabad 500 046, India

^b Department of Chemistry, School of Engineering, Dayananda Sagar University, Kudlu Gate, Bangalore 560 068, India

^c Organic Chemistry Division, CSIR-National Chemical Laboratory, Dr. Homi Bhabha Road, Pune 411 008, India

^d Department of Chemistry, Institute of Chemical Technology-Indian Oil Odisha Campus, IIT Kharagpur Extension Centre, Mouza Samantpuri, Bhubaneswar 751 013, Odisha, India

* Email: ashwini.nangia@gmail.com, anands-chem@dsu.edu.in.

Electronic Supplementary Information†

Table S1. Preparation of NFPD-FBA crystal forms by grinding in wet solvent slurry. See refs. 15,16 for details on preparation of NFPD salts and cocrystals.

Solid form	NFPD mg, (mmol)	Coformer mg, (mmol)	Type of method with organic solvent added	Selection of organic solvent for crystallization of NFPD-FBA
NFPD-BA	392 (0.1)	122 (0.1)	Mortar-pestle grinding with CH ₃ CN (1 mL)	MeOH (40 mg in 5 mL)
NFPD-3FBA	392 (0.1)	140 (0.1)	Mortar-pestle grinding with CH ₃ CN (1 mL)	MeOH (40 mg in 5 mL)
NFPD-34DFBA	392 (0.1)	158 (0.1)	Mortar-pestle grinding with CH ₃ CN (1 mL)	MeOH (40 mg in 5 mL)
NFPD-35DFBA	392 (0.1)	158 (0.1)	Mortar-pestle grinding with CH ₃ CN (1 mL)	MeOH (40 mg in 5 mL)
NFPD- 234TFBA	392 (0.1)	176 (0.1)	Mortar-pestle grinding with CH ₃ CN (1 mL)	MeOH (40 mg in 5 mL)
NFPD- 235TFBA	392 (0.1)	176 (0.1)	Mortar-pestle grinding with CH ₃ CN (1 mL)	MeOH (40 mg in 5 mL)
NFPD-	392 (0.1)	176 (0.1)	Mortar-pestle grinding with	MeOH (40 mg in 5 mL)

245TFBA			CH ₃ CN (1 mL)	
NFPD- 2356TFBA	392 (0.1)	194 (0.1)	Mortar-pestle grinding with CH ₃ CN (1 mL)	MeOH (40 mg in 5 mL)

Table S2 ΔpK_a values^a of benzoic acid, fluorobenzoic acid coformers and NFPD drug.

API/ Coformer	pK_a in water	ΔpK_a	Molecular complex
NFPD	7.34	---	---
3FBA	3.76	3.58	1:1 Salt
34DFBA	3.93	3.41	1:1 Salt
35DFBA	3.44	3.90	1:1 Salt
234TFBA	3.17	4.17	1:1 Salt
235TFBA	2.64	4.70	1:1 Salt
245TFBA	3.14	4.20	1:1 Salt
2356TFBA	1.84	5.50	1:1 Salt
BA	4.20	3.14	1:1 Salt

^a pK_a 's were calculated using Marvin 5.10.1, 2012, ChemAxon, <http://www.chemaxon.com>.

Table S3. FT-IR stretching frequency for COOH, COO⁻, NH/OH and aliphatic and aromatic CH peaks of NFPD and coformers.

S. No.	Compound	COOH, COO ⁻ ($\nu C=O$, cm^{-1})	alcohol/piperzinium ($\nu NH/OH$, cm^{-1})	Aliphatic and aromatic CH (νCH , cm^{-1})
1	NFPD	---	3438	3048, 3010, 2935, 2823
2	BA	1686	---	3073, 2834
3	NFPD–BA	1593	3406	3062, 2930, 2828
4	3FBA	1685	---	3003
5	NFPD–3FBA	1613	3402	3071, 2926, 2829
6	3,4DFBA	1688	---	3071
7	NFPD–3,4DFBA	1613	3395	3071, 2926, 2829

8	3,5DFBA	1692	---	3096
9	NFPD-3,5DFBA	1579	---	3050, 2924, 2832
10	2,3,4TFBA	1692	---	3092
11	NFPD-2,3,4TFBA	1594	---	3057, 2903, 2845
12	2,3,5-TFBA	1709	---	2924
13	NFPD-2,3,5TFBA	1614	---	3063, 3000, 2935, 2830
14	2,4,5-TFBA	1691	---	3078
15	NFPD-2,4,5TFBA	1619	---	3061, 2845
16	2,3,5,6-TFBA	1707	---	2924
17	NFPD-2,3,5,6TFBA	1614	3383	3063, 3003, 2935, 2830

The red shift in carbonyl peak ($\Delta\nu$ 60-100 cm^{-1}) is indicative of COOH to COO^- transformation.

Table S4. Crystallographic parameters of NFPD salts. Crystal data on NFPD-BA salt is reported in ref. 16.

Compound	NFPD-3FBA	NFPD-34DFBA	NFPD-35DFBA	NFPD-234TFBA	NFPD-235TFBA	NFPD-245TFBA	NFPD-2356TFBA
Emp. form.	C ₂₄ H ₂₉ N ₂ O ₃ , C ₇ H ₃ F O ₂	C ₂₄ H ₂₉ N ₂ O ₃ , C ₇ H ₃ F ₂ O ₂	C ₂₄ H ₂₉ N ₂ O ₃ , C ₇ H ₃ F ₂ O ₂	C ₂₄ H ₂₉ N ₂ O ₃ , C ₇ H ₂ F ₃ O ₂	C ₂₄ H ₂₈ N ₂ O ₃ , C ₇ H F ₃ O ₂	C ₂₄ H ₂₉ N ₂ O ₃ , C ₇ F ₃ O ₂	C ₂₄ H ₂₉ N ₂ O ₃ , C ₆ H ₄ N O ₂
Form. Wt.	532	550	550	568	568	568	586
Cryst. Syst.	Monoclinic	Monoclinic	Monoclinic	Monoclinic	Monoclinic	Monoclinic	Monoclinic
Space group	$P2_1/c$	$P2_1/c$	$P2_1/c$	$P2_1/c$	$P2_1/c$	$P2_1/c$	$P2_1/c$
T (K)	293	293	293	293	293	293	293
a (Å)	11.1975(5)	11.0504(6)	11.7664(8)	10.6351(9)	11.700(2)	10.760(3)	11.3702(5)
b (Å)	17.7650(8)	17.8882(9)	11.2033(8)	24.357(2)	16.998(3)	24.632(9)	19.8859(8)
c (Å)	13.5020(6)	13.3766(6)	21.4616(16)	11.6532(9)	13.643(2)	11.501(4)	12.9822(6)
α (°)	90	90	90	90	90	90	90
β (°)	96.456(2)	96.629(2)	96.300(3)	116.275(3)	99.744(8)	116.48(1)	100.236(2)
γ (°)	90	90	90	90	90	90	90

Z	4	4	4	4	4	4	4
V (Å ³)	2668.8 (2)	2626.5(2)	2812.0(3)	2706.8(4)	2674.1(8)	2728.4(16)	2888.6(2)
Density g cm ⁻³	1.321	1.392	1.291	1.395	1.407	1.379	1.346
RfIns. Collect	40373	142326	44281	89112	81031	78146	102449
Unique RfIns.	4736	21885	4980	13098	8109	10332	5958
Obsd. RfIns.	3602	15915	4007	8487	7506	6221	3522
Parameters	486	443	498	375	394	390	391
R ₁	0.0489	0.0664	0.0575	0.0583	0.0550	0.0645	0.0702
wR ₂	0.1349	0.1864	0.1598	0.1547	0.1726	0.1694	0.1633
GOF	1.031	1.101	1.045	1.041	1.256	1.025	1.116
Diffractionmeter	BRUKER	BRUKER	BRUKER	BRUKER	BRUKER	BRUKER	BRUKER

Table S5. Melting point of NFPD, salt and coformers

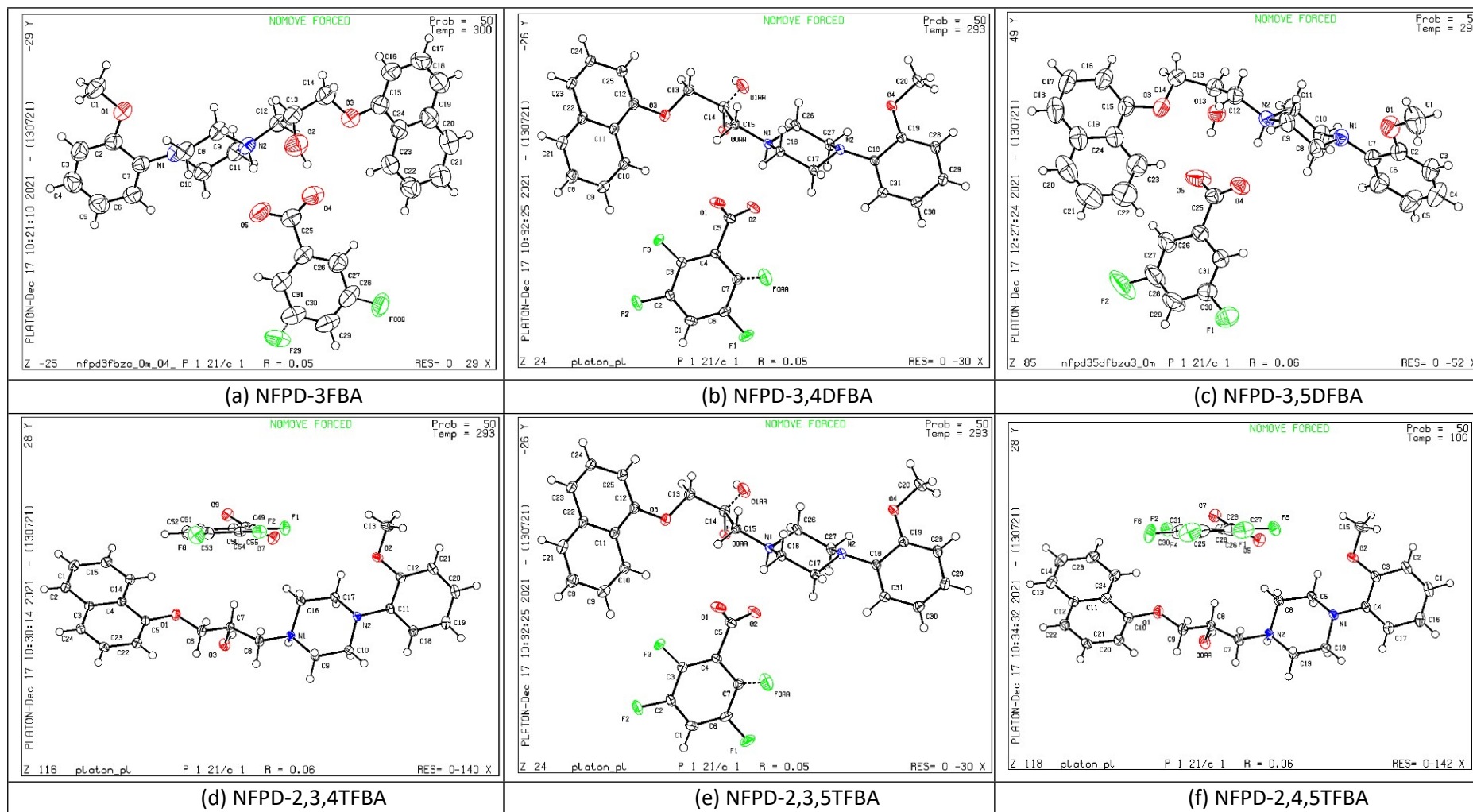
S. No.	Salts	m.p. range (°C)	Coformer	m.p. range (°C)
1	NFPD	125-127	---	---
2	NFPD-BA	145-149	BA	119-123
3	NFPD-3FBA	146-147	3FBA	124-131
4	NFPD-34DFBA	122-124	3,4DFBA	120-124
5	NFPD-35DFBA	147-148	3,5DFBA	121-124
6	NFPD-234TFBA	134-136	2,3,4TFBA	140-144
7	NFPD-235TFBA	140-141	2,3,5TFBA	107-112
8	NFPD-245TFBA	121-123	2,4,5TFBA	96-100
9	NFPD-2356TFBA	163-165	2,3,5,6TFBA	148-152

Table S6. Initial pH value of the dissolution medium and post 8 h dissolution medium pH.

	pH value at start of dissolution	pH value after 8 h dissolution
NFPD–3FBA	6.74	6.45
NFPD–34DFBA	6.75	6.31
NFPD–35DFBA	6.76	6.34
NFPD–234TFBA	6.74	6.29
NFPD–235TFBA	6.74	6.24
NFPD–245TFBA	6.78	6.28
NFPD–2356TFBA	6.74	6.18
NFPD–BA	6.76	6.48
NFPD	6.75	6.85

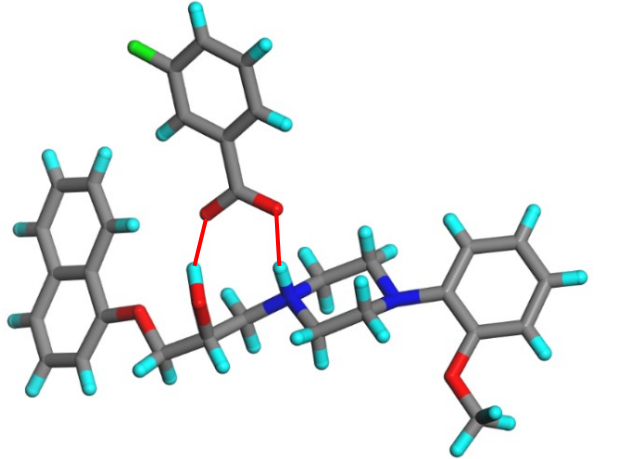
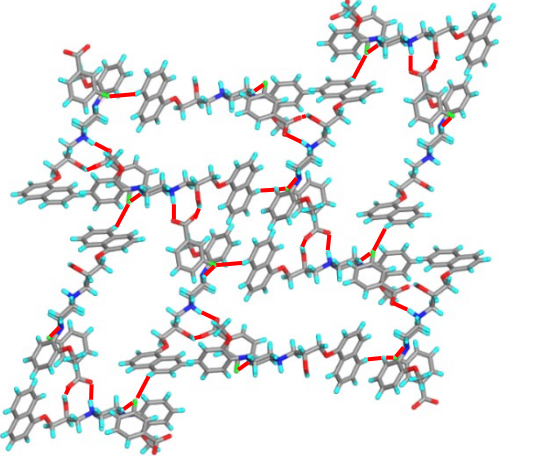
Table S7. Calculated log *P* (Marvin Chemaxon) and experimental permeability performance value of NFPD–FBA salts.

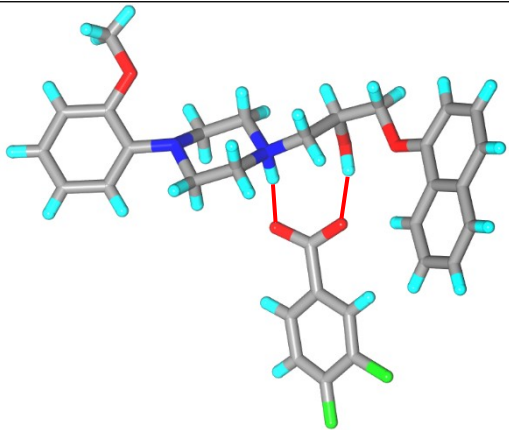
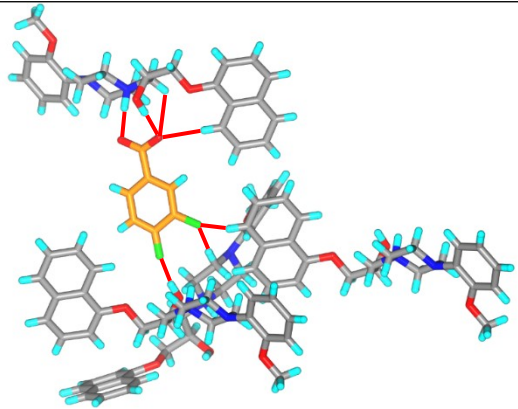
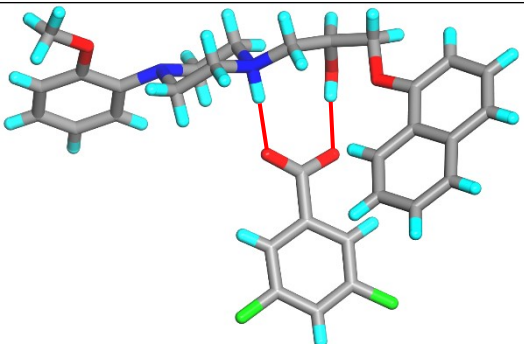
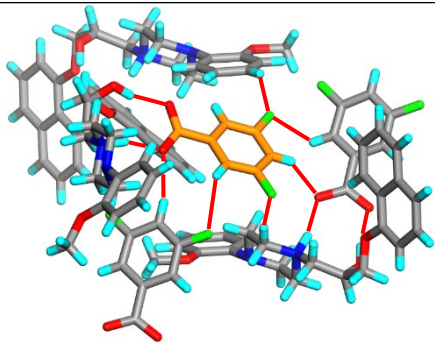
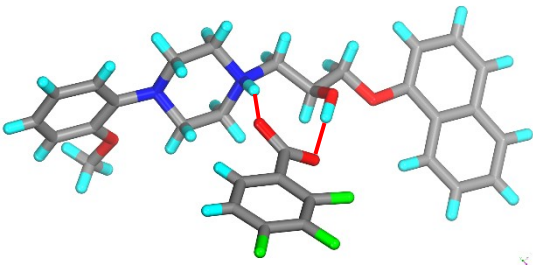
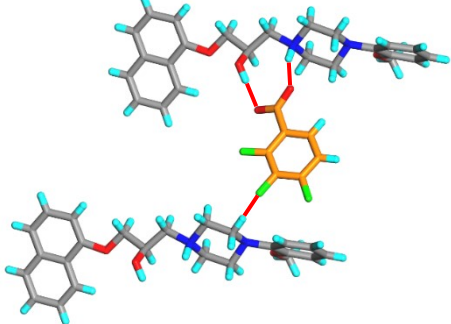
Name	logP API/coformer	Perm of Salts Peak flux value $\mu\text{g}\cdot\text{cm}^2\cdot\text{h}^{-1}$	Perm of Salts AUC flux 0-8 h $(\mu\text{g}\cdot\text{cm}^2\cdot\text{h}^{-1})$
NFPD (pure drug)	3.77	1.75	8.87
NFPD-BA	1.63	2.61	12.70
NFPD-3FBA	1.77	4.63	21.54
NFPD-3,4FBA	1.92	5.01	24.79
NFPD-3,5FBA	1.92	4.99	23.36
NFPD-2,3,4TFBA	2.06	5.03	27.45
NFPD-2,3,5TFBA	2.06	4.45	20.81
NFPD-2,4,5TFBA	2.06	5.48	35.46
NFPD-2,3,5,6TFBA	2.20	7.96	45.95

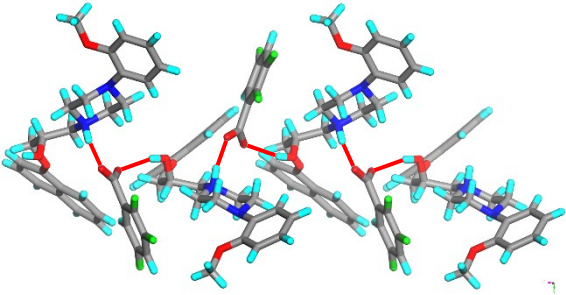
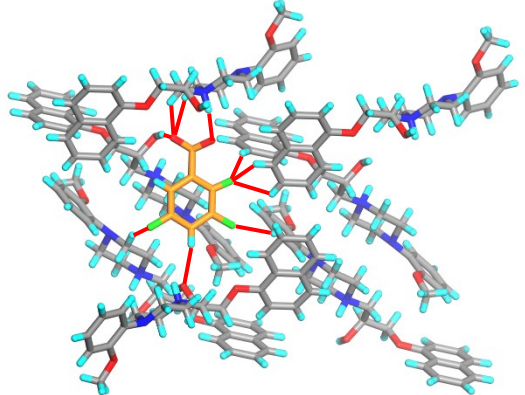
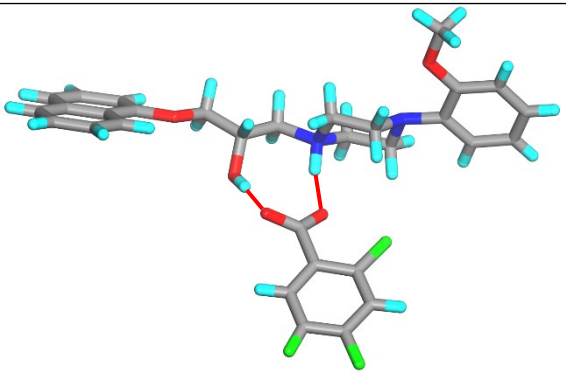
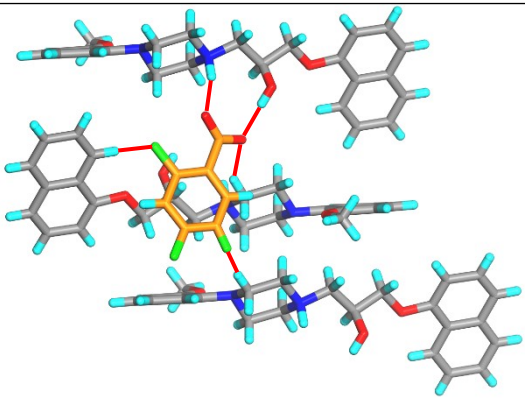


		
(g) NFPD-2,3,5,6TFBA		

Figure S1. (a-g) ORTEP diagrams at 50% probability of electron density ellipsoids for heavy atoms in NFPD-FBA binary products. The COO⁻ and piperazine-NH⁺ groups are clearly visible in this figure and the packing diagrams (next figure).

<p>NFPD-3FBA</p> <p>Cyclic synthon I of N-H...O⁻ and O-H...O⁻ hydrogen bonds</p> <p>Hydrogen bonded 2D corrugated layer structure formed via auxiliary C-H...F interactions with the hydrogen-bonded ring synthons of NFPD and 3FBA</p>		
---	---	--

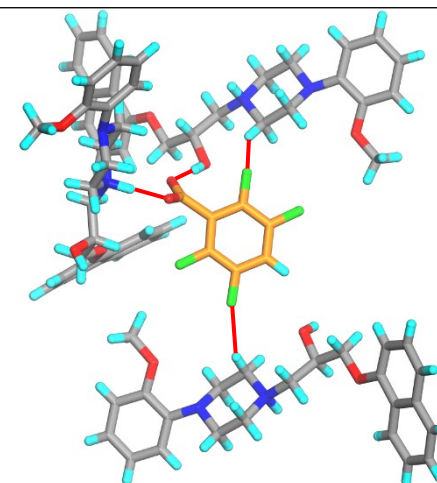
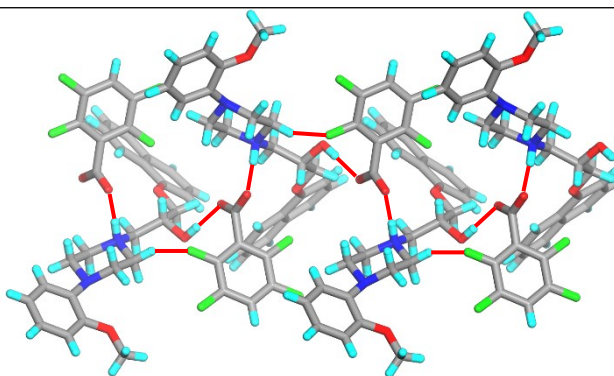
<p>NFPD–34DFBA</p> <p>Cyclic synthon I of $\text{N-H}\cdots\text{O}^-$ and $\text{O-H}\cdots\text{O}^-$ hydrogen bonds</p> <p>Hydrogen bonding of 34DFBA with adjacent NFPDH surrounding ions</p>		
<p>NFPD–35DFBA</p> <p>Cyclic synthon I of $\text{N-H}\cdots\text{O}^-$ and $\text{O-H}\cdots\text{O}^-$ hydrogen bonds</p> <p>Hydrogen bonding of 35DFBA with adjacent NFPDH surrounding ions</p>		
<p>NFPD–234TFBA</p> <p>Cyclic synthon I of $\text{N-H}\cdots\text{O}^-$ and $\text{O-H}\cdots\text{O}^-$ hydrogen bonds</p> <p>Hydrogen bonding of 234TFBA with adjacent NFPDH ion</p>		

<p>NFPD–235TFBA</p> <p>Chain synthon II of $\text{N-H}\cdots\text{O}^-$ and $\text{O-H}\cdots\text{O}^-$ hydrogen bonds</p> <p>Hydrogen bonding of 235TFBA with adjacent surrounding NFPDH ion</p> <p>The drug OH group has two positions (s.o.f. 0.75:0.25) and the coformer is disordered over two orientations (0.85:0.15) in the crystal structure refined to the lowest R-factor. Due to disorder the tri-fluorobenzoic acid coformer mimics pentafluorobenzoic acid (central molecule in right side structure)</p>		
<p>NFPD–245TFBA</p> <p>Cyclic synthon I of $\text{N-H}\cdots\text{O}^-$ and $\text{O-H}\cdots\text{O}^-$ hydrogen bonds</p> <p>Hydrogen bonding of 245TFBA with adjacent NFPDH ion</p>		

NFPD–2356TFBA

Chain synthon II of $\text{N-H}\cdots\text{O}^-$ and $\text{O-H}\cdots\text{O}^-$ hydrogen bonds

Hydrogen bonding of 235TFBA with adjacent surrounding NFPDH ion



NFPD–BA

Cyclic synthon I of $\text{N-H}\cdots\text{O}^-$ and $\text{O-H}\cdots\text{O}^-$ hydrogen bonds

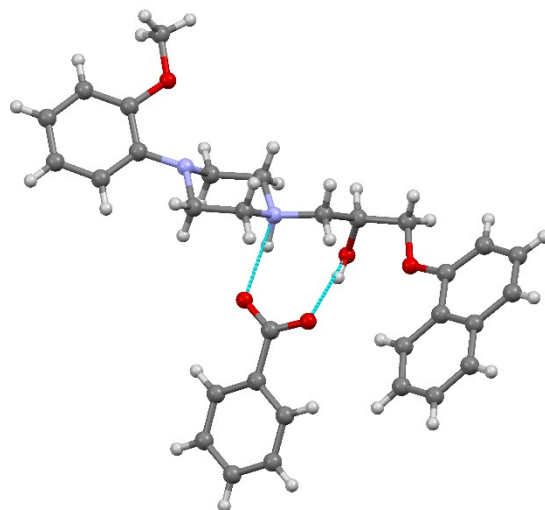
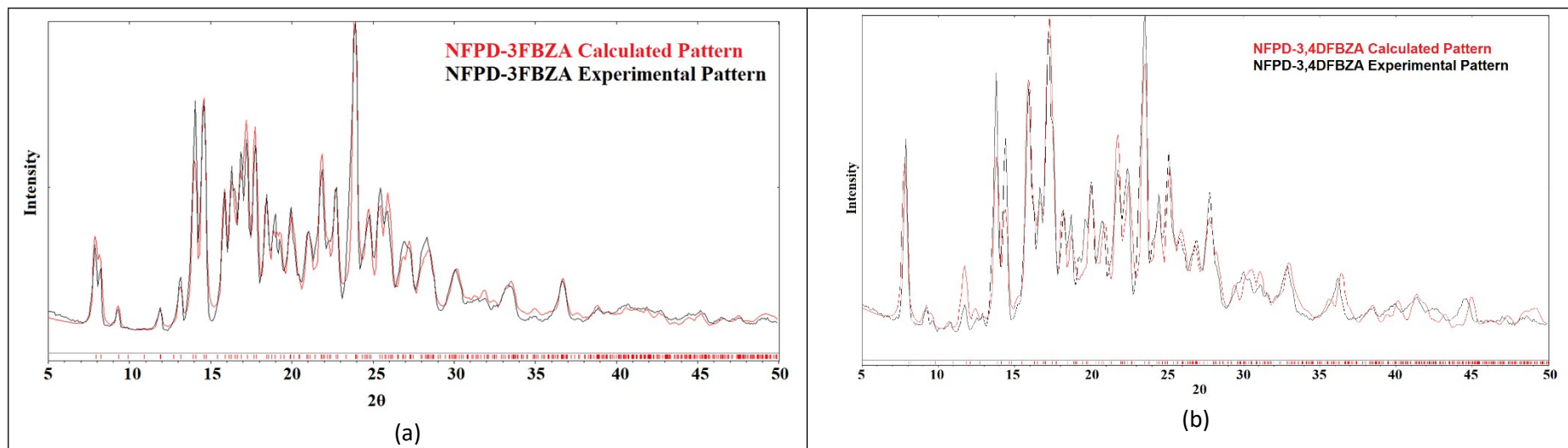
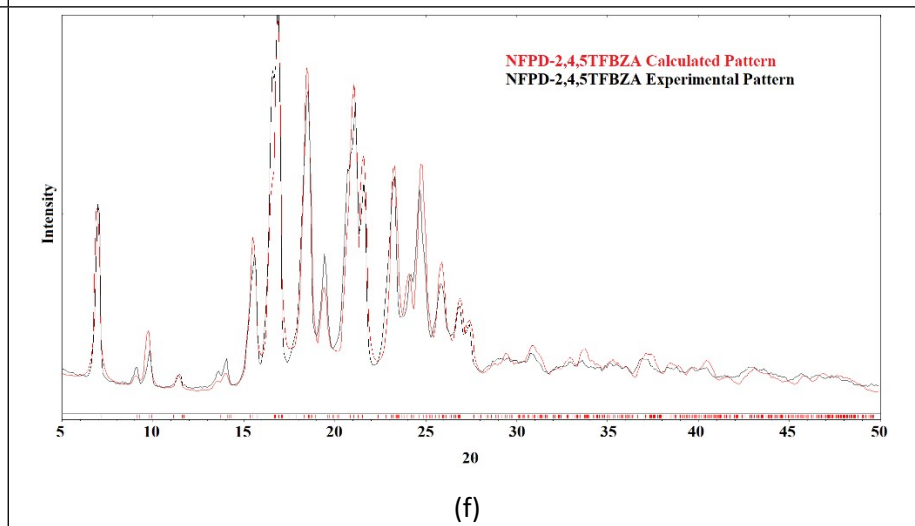
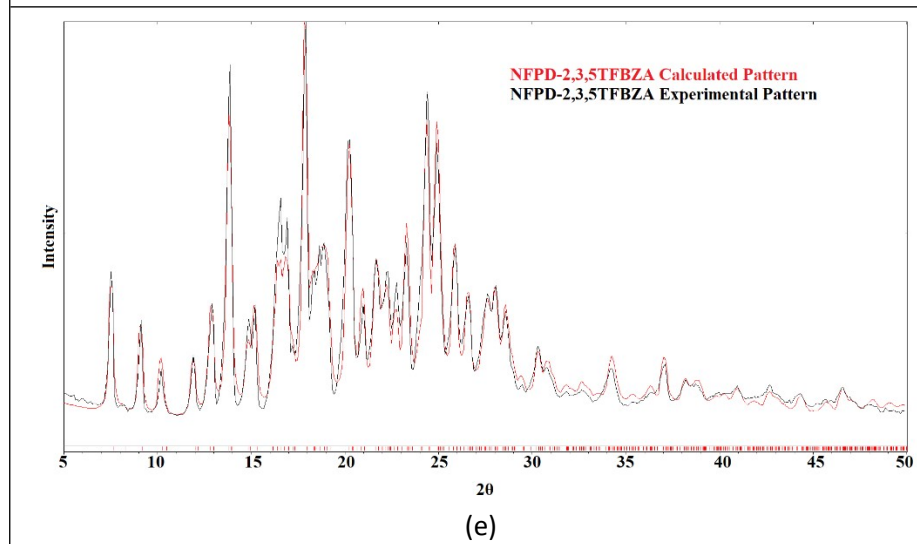
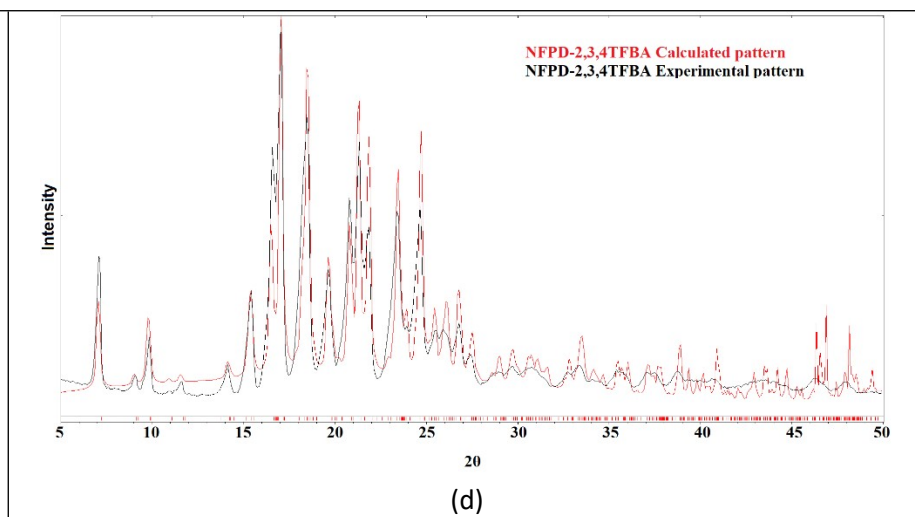
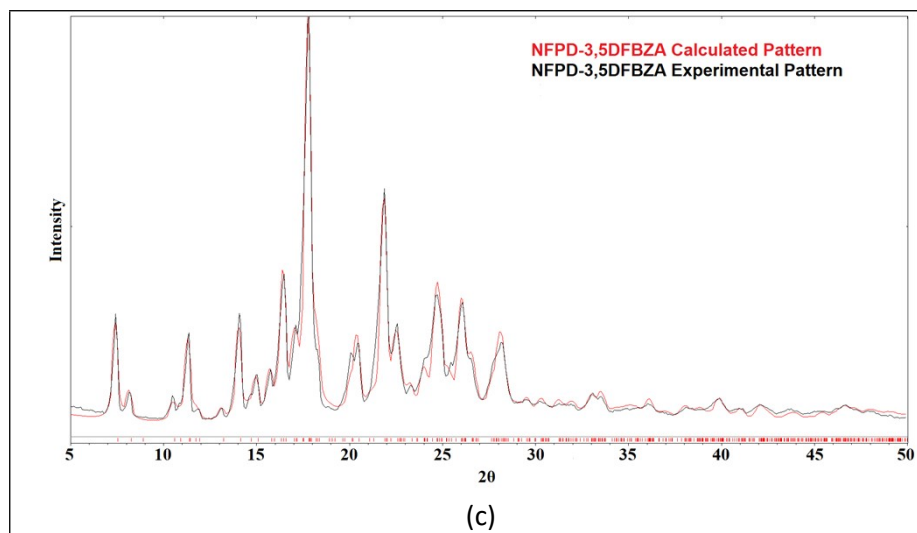


Figure S2. Crystal packing diagrams of NFPD-FBA salts. The primary synthon and one hydrogen bonded structure portion are shown in each case. C—H...F interactions where relevant are shown as dashed lines.

Analysis of hydrogen bonding synthons in these crystal structures suggests that after a certain degree of fluorination on benzoic acid (pentafluoro) there is a shift in heterosynthon from cyclic (I) to chain (II). 235TFBA salt has the chain synthon even though it is tri-fluorinated because in the crystal structures the coformer resembles a pentafluoro phenyl group due to disorder, as shown above.





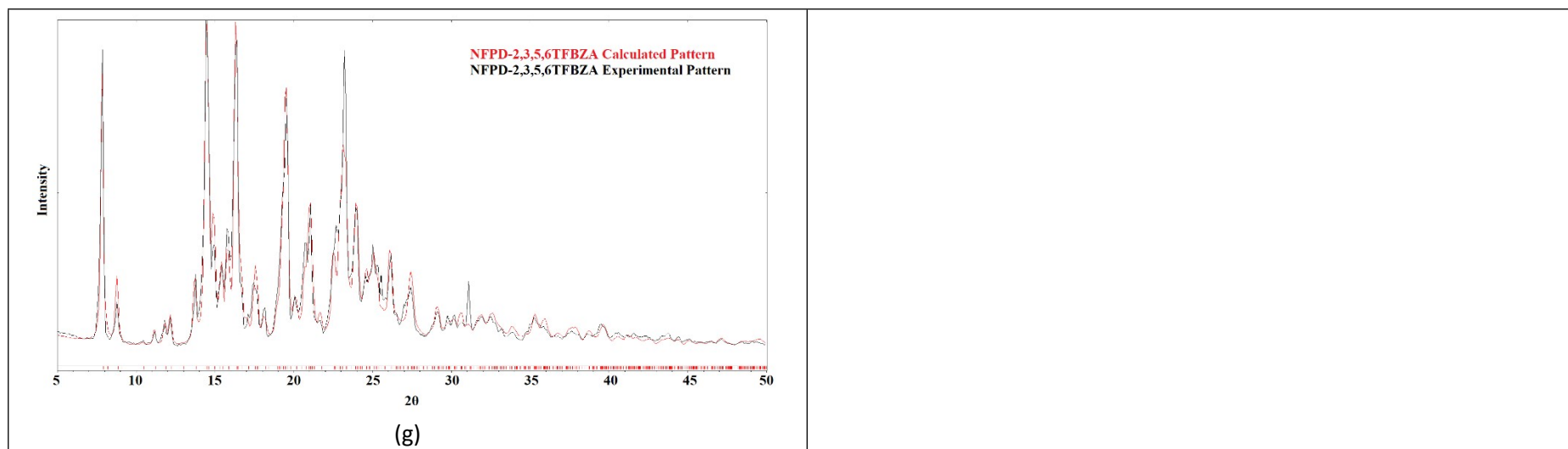
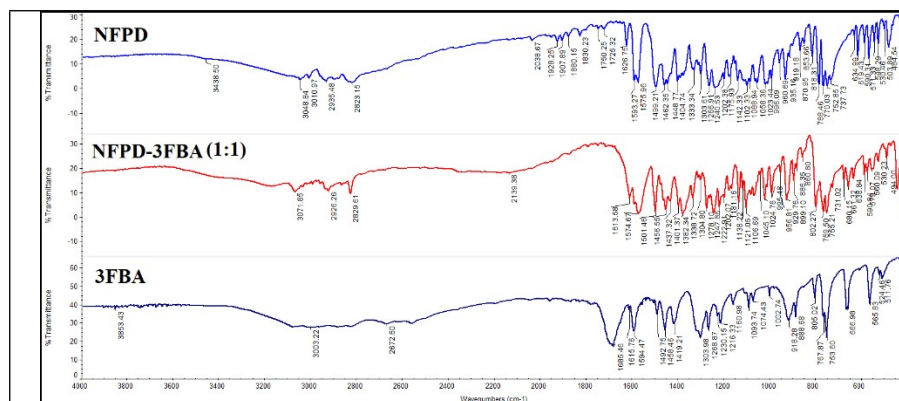
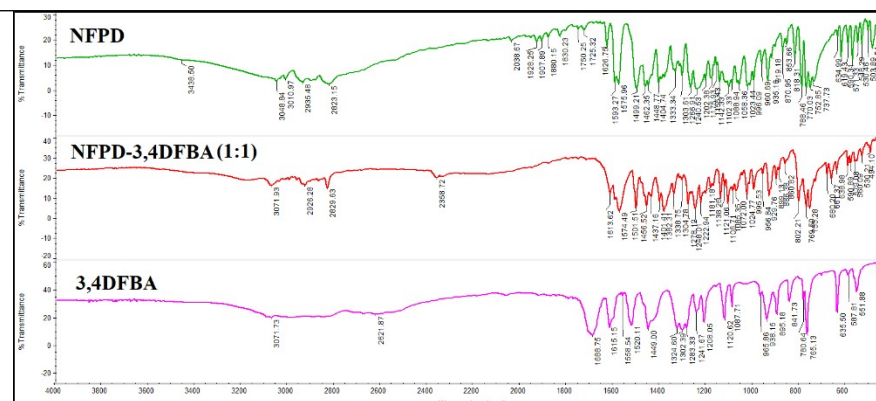


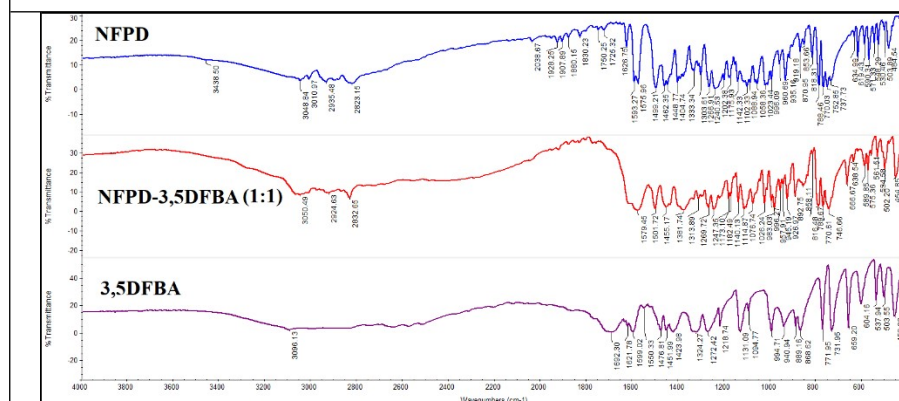
Figure S3. Experimental PXRD pattern of NFPD–FBA salts (black) show excellent match with the calculated line profile from the calculated X-ray crystal structure (red), indicating bulk purity and phase homogeneity. (a) Rietveld refinement for NFPD–3FBA gave $R_p = 0.857$, $R_{wp} = 0.1111$, and $R_{exp} = 0.9394$. (b) Rietveld refinement for NFPD–34DFBA gave $R_p = 0.115$, $R_{wp} = 0.1612$, and $R_{exp} = 0.6101$. (c) Rietveld refinement for NFPD–35DFBA gave $R_p = 0.910$, $R_{wp} = 0.1295$, and $R_{exp} = 0.1134$. (d) Rietveld refinement for NFPD–234TFBA gave $R_p = 0.125$, $R_{wp} = 0.1819$, and $R_{exp} = 0.8784$. (e) Rietveld refinement for NFPD–235TFBA gave $R_p = 0.825$, $R_{wp} = 0.1031$, and $R_{exp} = 0.3775$. (f) Rietveld refinement for NFPD–245TFBA gave $R_p = 0.1269$, $R_{wp} = 0.1986$, and $R_{exp} = 0.7082$. (g) Reitveld refinement for NFPD–2356DFBA gave $R_p = 0.1210$, $R_{wp} = 0.1616$, and $R_{exp} = 0.1366$.



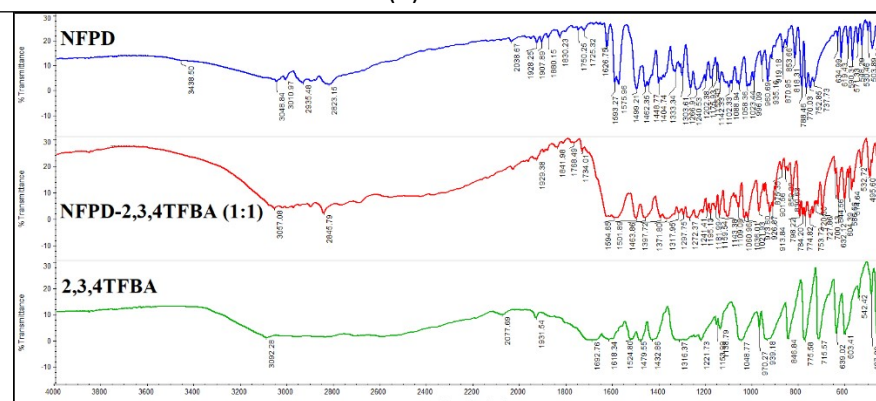
(a) 3FBA



(b) 34DFBA



(c) 35DFBA



(d) 234TFBA

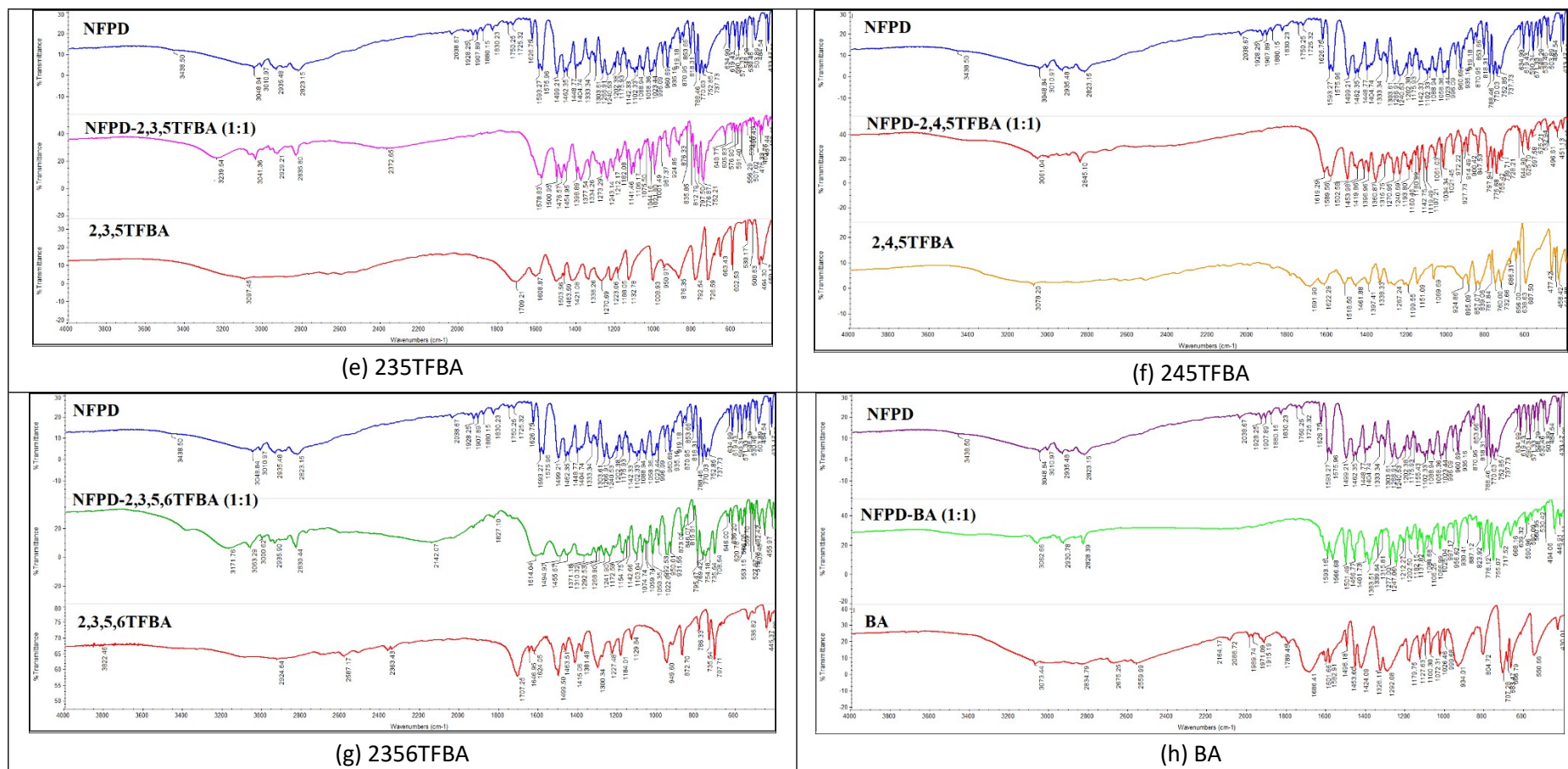
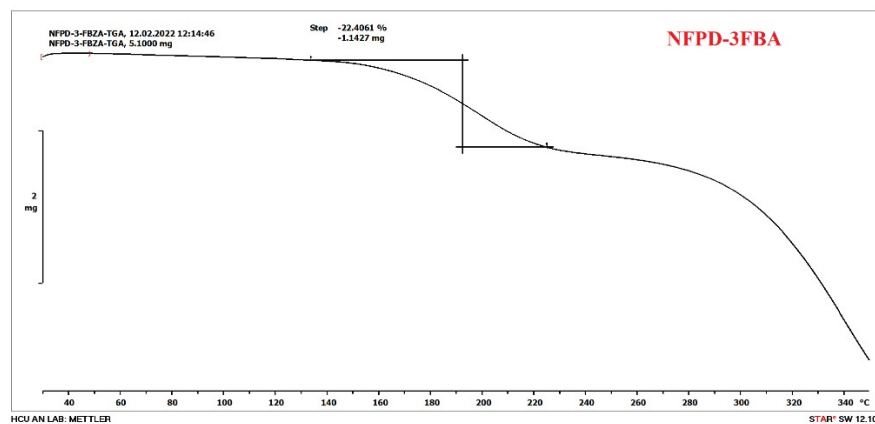
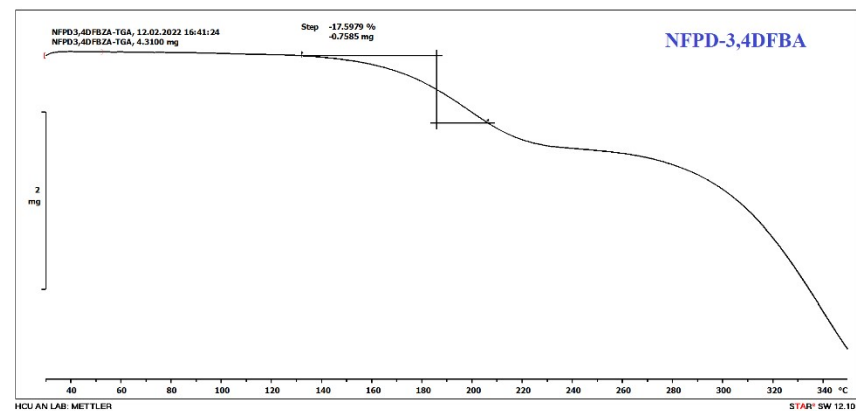


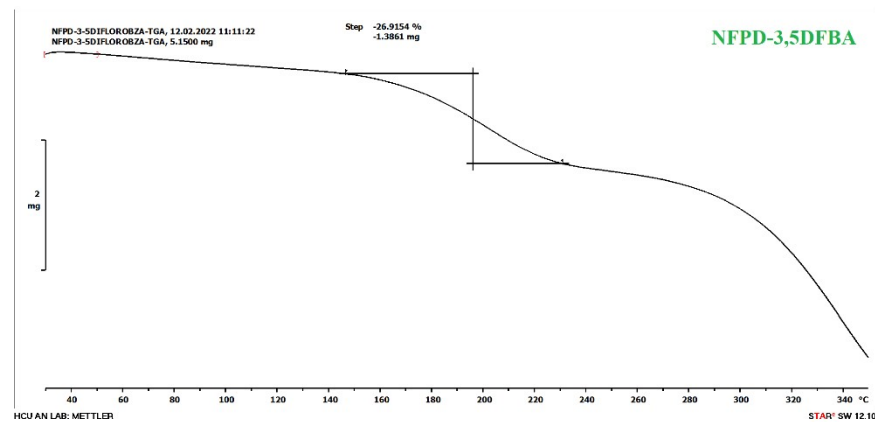
Figure S4. IR spectra of NFPD–FBA salts compared with the starting materials.



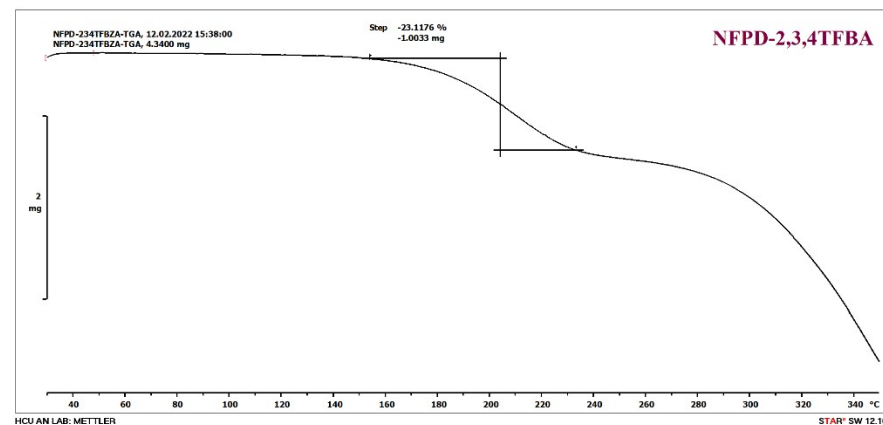
(a) 3FBA



(b) 34DFBA



(c) 35DFPA



(d) 234TFBA

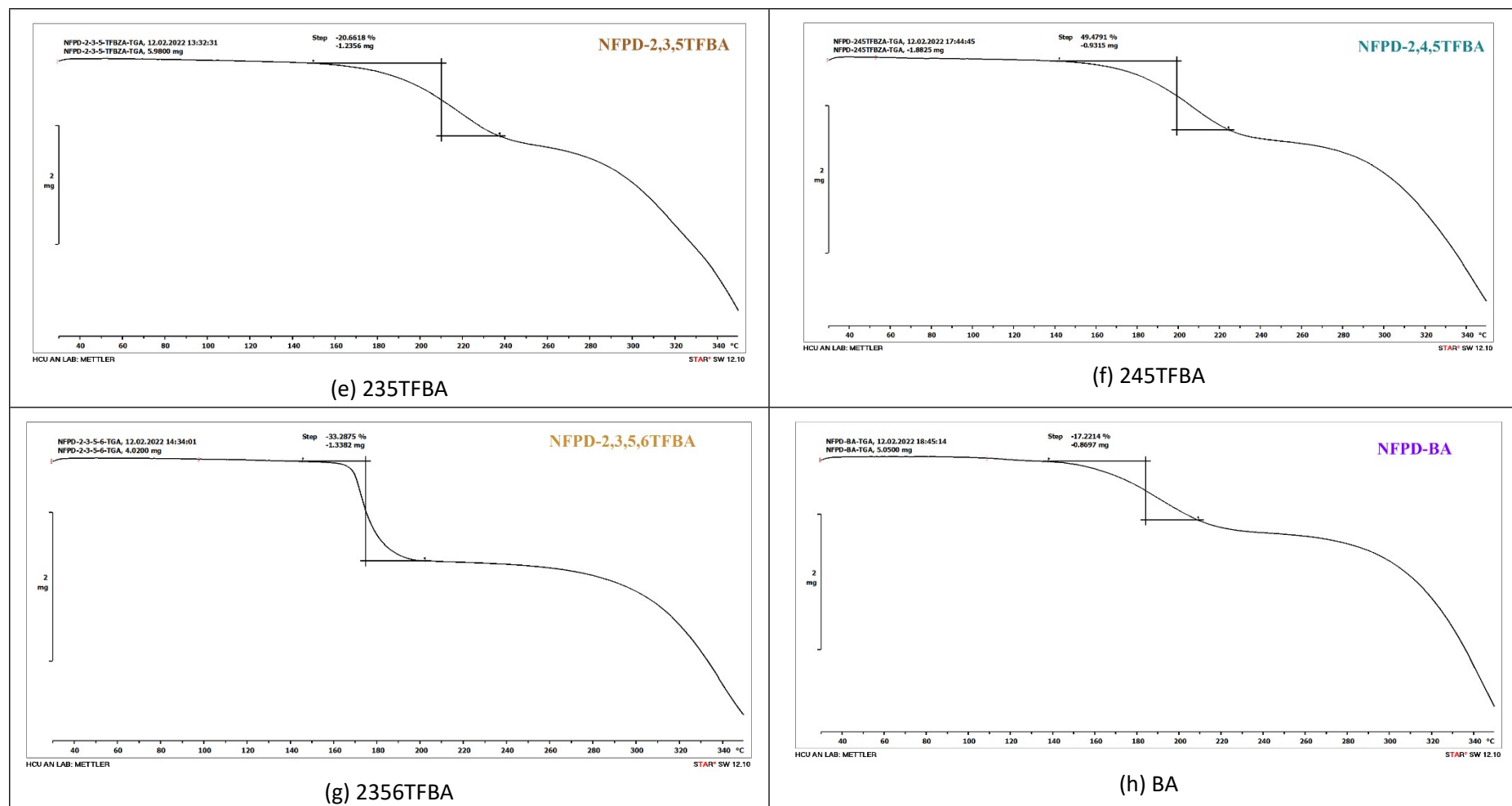


Figure S5. TGA plots of NFPD–FBA salts show weight loss after the melting point of the drug and/ or the coformer, typically > 140 °C.

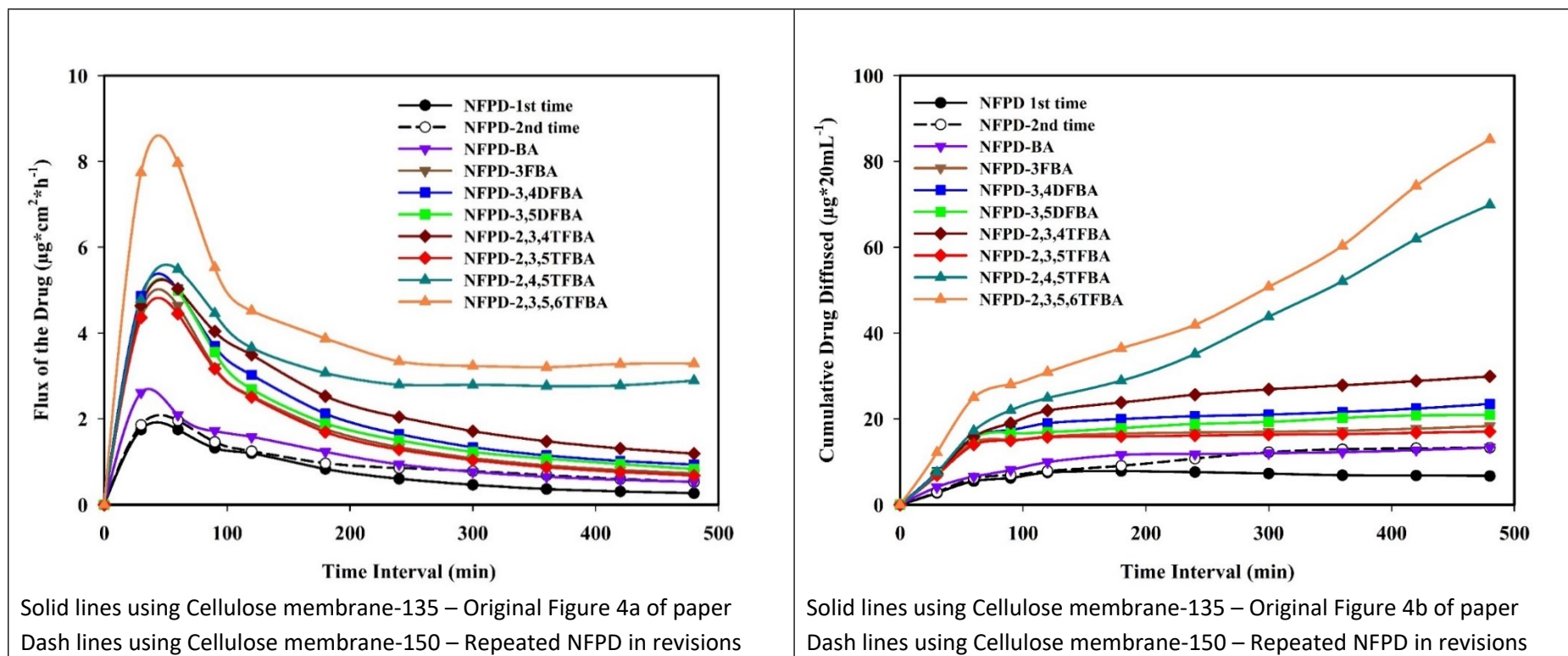


Figure S6. Repeat of NFPD permeability using Cellulose membrane-150 (dash lines) shows higher values of drug concentration in both plots.

Experimental Details

Crystal form Characterization

Few single crystals obtained after crystallization were mounted on a Super Nova Dual Source X-ray Diffractometer (Rigaku OD) system equipped with a CCD area detector and the X-ray generator was operated at 50 kV and 0.8 mA to generate Mo-K α radiation ($\lambda = 0.71073 \text{ \AA}$) or Cu-K α radiation ($\lambda = 1.54178 \text{ \AA}$) at 293(2) K. Data reduction was performed using CrysAlisPro 171.33.55 software (CrysAlisPro; 2010). Bruker APEX II, CCD diffractometer, Mo-K α ($\lambda = 0.71073 \text{ \AA}$) radiation was used to collect X-ray reflections of remaining crystals. Bruker D8 Quest diffractometer equipped with a graphite monochromator and Mo-K α fine-focus sealed tube ($\lambda = 0.71073 \text{ \AA}$) and deduction was performed using APEX-II software. Intensities for absorption were corrected with SADABS and the

crystal structures were solved and refined using SHELXL-97 with anisotropic displacement parameters for non-H atoms. Hydrogen atoms on O and N were experimentally located in all crystal structures. Hydrogen atoms were experimentally located through the Fourier difference electron density maps in all crystal structures. All O–H and C–H atoms were fixed geometrically with HFIX command in SHELX-TL program of Bruker-AXS. Crystal parameters shown in (Table S4). A final check CIF was carried out using PLATON for any missed symmetry. X-Seel was used to prepare packing diagrams. Crystallographic .cif files are available at www.ccdc.cam.ac.uk/data such as part of the Supporting Information (CCDC Nos. 2130416-2130422).

Powder X-ray diffraction

PXRD was recorded on Bruker D8 Advance diffractometer (Bruker-AXS, Karlsruhe, Germany) with Cu-K α radiation of $\lambda = 1.5406 \text{ \AA}$ and an acceleration voltage of 40 kV and current of 30 mA power. API NFPD and its fluorobenzoic acid salts were scanned in the reflectance mode range from 5° to 50° (2 θ) at scan rate of 5°/min.

Vibrational spectroscopy

Infrared spectra of NFPD and its FBA salts were acquired by FT-IR spectroscopy (Thermo-Nicolet 6700 FT-IR spectrometer (Thermo Scientific, Waltham, MA) with the samples spread in KBr pellets and Omnic software (Thermo Scientific, Waltham, MA) was utilized to analyze the data. Each sample was scanned in the range of 400–4000 cm⁻¹, and the spectra were normalized with the background correction.

Thermal analysis

DSC were recorded on Mettler-Toledo DSC 822e module (Mettler-Toledo, Columbus, OH) to record the melting point. TGA was carried out on Mettler Toledo TGA/SDTA 851e module (Mettler-Toledo, Columbus, OH) to measure any weight loss from the crystalline solid. NFPD salts were placed in a sealed pin-pricked aluminum pan for DSC experiments. The characteristic sample size is 3-5 mg for DSC and 4-6 mg for TGA. The temperature range for the heating curves was 30-350 °C, and the sample was heated at a rate of 10 °C/ min. All the samples were purged in a stream of dry nitrogen flowing at 80 mL/min.

Solubility and dissolution measurements

Solubility measurements of API NFPD and its fluoro salts were conducted in a pH 7 phosphate-buffered saline (PBS) medium. The absorbance of NFPD was measured at λ_{max} of 282 nm in purified buffer solution of pH 7 PBS medium by high-performance liquid chromatography (HPLC) analysis. The concentration versus intensity calibration curve was plotted by using these absorbance values, which were obtained from the known concentration of pure NFPD. A molar extinction coefficient for NFPD was calculated from the slope of the calibration curve. To measure the equilibrium solubility, an excess amount of each sample (i.e., pure NFPD and its FBA salt) was added to 5 mL of purified buffer in PBS medium at pH 7 and stirred at 800 rpm using a magnetic stirrer at 37 °C \pm 1 to make the solution saturated. After 24 h, the suspension was filtered through a Whatman 0.45 μm syringe filter. The filtrate was used to calculate the equilibrium solubility from the area under curve (AUC) plotted against the standard curve. The undissolved residues were air-dried and further characterized by PXRD.

Electrolab TDT-08L dissolution tester is used to perform powder dissolution (PD) studies. The powder dissolution measurements were performed using NFPD 200 mg and this mass of active drug was consistently used for reference salt NFPD-BA (262 mg) and for the FBA salts: NFPD-3FBA (271 mg), NFPD-34DFBA (280 mg), NFPD-35DFBA (280 mg), NFPD-234TFBA (289 mg), NFPD-235TFBA (289 mg), NFPD-245TFBA, (289 mg), and NFPD-2356TFBA (299 mg) amount which was taken into 500 mL of pH 7 phosphate buffer saline (PBS) dissolution medium. The paddle shaft rotation was fixed at 100 rpm and dissolution experiments were continued up to 8 h at 37 °C. At regular intervals, 5 mL of the dissolution medium was withdrawn and replaced by an equal volume of fresh medium to maintain a constant volume and the concentration of the aliquots was quantified by HPLC at 282nm λ_{max} and was calculated by the linear trapezoidal method from 0 to 8 h.

Diffusion Measurements

Diffusion studies are carried out with glass Franz diffusion cell (Model JFDC-07, Orchid Scientific, Maharashtra, India) with a 20 mL volume. The membrane used here are cellulose membrane-135 (width 33.12 mm, and diameter 23.8 mm, capacity 4.45 mL/cm) are purchased from HiMedia, India. The cellulose membrane was pre-treated with 2% NaHCO₃ at 80 °C for 30 min to remove traces of sulfides, followed by 10 mM of EDTA at 80 °C for 30 min to remove traces of heavy metal and another 30 min of treatment with deionized water at 80 °C to remove glycerin. The treated membrane was placed between the two compartments fixed by a stainless-steel clamp with an effective mass transfer area of 3.14 cm². The receptor compartment is filled with PBS solution, and air bubbles are removed. The next, donor compartment is loaded with 20 mg API NFPD and its fluoro salts in equimolar ratio powders (20 mg active NFPD drug was maintained in all experiments) and 2 mL of PBS were added. The temperature of diffusion medium is thermostatically maintained at 37±1 °C throughout the experiment at 600 rpm and permitted to diffuse through the membrane towards the receptor compartment. Aliquots of 0.5 mL are withdrawn from the receptor compartment at set time periods (30, 60, 90, 120, 180, 240, 300, 360, 420, 480 min) and fresh PBS was added to replenish volume. The diffused concentration was determined by HPLC.

HPLC assay

Shimadzu LC-20AD liquid chromatography, photodiode array SPD-M20A detector, and degasser DGU-20A3 are performed using reverse-phase (RP) HPLC column C18G (250 × 4.6 mm, 5 μ m particle size). UV absorbance at 282 nm was used to quantify the NFPD drug. The calibration curves are obtained by spiking NFPD (linearity R² > 0.999). The mobile phase consists of 10 mM ammonium acetate buffer-acetonitrile (40:60) and adjusted to pH 4 by glacial acetic acid, which is filtered through a 0.45 μ m membrane filter, degassed by a sonicator, and delivered at a rate of 1 mL/min. The solubility, dissolution, and diffusion samples were injected into HPLC with a run time of 15 min.

Selection of permeability method

Different membranes have been used for permeability passage studied,¹ and cellulose nitrate membrane is quite popular and used in several of the recently published papers²⁻⁶ which used cellulose membranes and we have followed a similar protocol. Apart from Franz cell diffusion cells (used in our study) other methods are PAMPA (Parallel Artificial membrane permeability Assay) which is similar to Franz cell and another option is with Caco2 cells permeability studies.

While there are different methods used to compare permeability and flux of drugs, the methods used in the present study provide an accurate comparison of the NFPD–FBA salts in analyzing the improvement of dissolution and permeability as a proof of principle study.

A review opined that NFPD drug exhibits permeability curve at the base line in the experimental period of 2-8 h (for cumulative drug diffused) except for the initial 120 min, and hence the receptor medium does not meet sink conditions. We thank the reviewer for this suggestion and repeated the experiment on NFPD with larger porosity cellulose membrane so that drug flux will be higher and faster. The repeat experimental additional plot overlayed on Figure 4 of the main paper is shown in Figure S6, to show the now higher passage of NFPD. Other salts will be recalibrated and detailed studies reported in a full article. The membrane used in the original experiments is: Cellulose membrane-135, Av. flat width - 33.12 mm, Av. Diameter - 23.8 mm, Capacity approx. - 4.45 mL/cm. The membrane used in the revision experiment is: Cellulose membrane-150, Av. flat width - 37.70 mm, Av. Diameter - 25.4 mm, Capacity approx.- 5.07 mL/cm. Thus, the larger pore diameter cellulose membrane shows higher cross-over to the receptor compartment of the drug and a gradual increase in cumulative drug diffused with time.

1. S.-F. Ng, J. Rouse, D. Sanderson, and G. Eccleston, A Comparative Study of Transmembrane Diffusion and Permeation of Ibuprofen across Synthetic Membranes Using Franz Diffusion Cells. *Pharmaceutics*, 2010, **2**, 209–223.
2. M. Banik, S. P. Gopi, S. Ganguly, and G. R. Desiraju, Cocrystal and Salt Forms of Furosemide: Solubility and Diffusion Variations. *Cryst. Growth Des.*, 2016, **16**, 5418–5428.
3. S. P. Gopi, S. Ganguly, and G. R. Desiraju, A Drug–Drug Salt Hydrate of Norfloxacin and Sulfathiazole: Enhancement of in Vitro Biological Properties via Improved Physicochemical Properties, *Mol. Pharmaceutics*, 2016, **13**, 3590–3594.
4. R. Khatioda, B. Saikia, P. J. Das, and B. Sarma, Solubility and in vitro drug permeation behavior of ethebamide cocrystals regulated in physiological pH environments, *CrystEngComm*, 2017, **19**, 6992–7000.
5. L.-Y. Wang, F.-Z. Bu, Y.-T. Li, Z.-Y. Wu, and C.-W. Yan, A Sulfathiazole–Amantadine Hydrochloride Cocrystal: The First Codrug Simultaneously Comprising Antiviral and Antibacterial Components, *Cryst. Growth Des.*, 2020, **20**, 3236–3246.
6. M. Guo, K. Wang, N. Qiao, V. Yardley, and M. Li, Investigating Permeation Behaviour of Flufenamic Acid Cocrystals using A Dissolution and Permeation System, *Mol. Pharmaceutics*, 2018, **15**, 4257–4272.